Random Roughness Enhances Lift in Supersonic Flow

Guang Lin,* Chau-Hsing Su,† and George Em Karniadakis‡

Division of Applied Mathematics, Brown University, Providence, Rhode Island 02912, USA

(Received 5 April 2007; published 5 September 2007)

We study the scattering of shock waves by a rough wedge using second-order perturbation analysis and stochastic simulations employed synergistically to cover a large range in correlation length A and amplitude ϵ of the profile roughness (with length d). For small ϵ and $A/d \ll 1$, the mean of the perturbed pressure scales $\propto \epsilon^2$ and $\propto (A/d)^{-2}$, while the corresponding variance scales $\propto \epsilon$ and $\propto (A/d)^{-1}$. However, for large ϵ, the mean pressure scales approximately $\propto \epsilon$, while for $A/d > 1$ it is independent of A. Our results are useful in evaluating the effects of roughness in high-speed flight but also in designing novel enhanced-lift aerodynamic surfaces using rough skin concepts.

DOI: 10.1103/PhysRevLett.99.104501 PACS numbers: 47.40.Ki, 46.65.+g

The reflection of a shock by a wedge is a fundamental problem in high-speed aerodynamics and has been studied extensively [1–4]. Assuming a smooth wedge surface and inviscid dynamics, the shock path and pressure distribution can be obtained by simple analytical formulas [5]. However, considering the wedge surface to be rough leads to complex shock dynamics that involves the interaction of multiple shocks and Mach waves. M. J. Lighthill [6] and B.-T. Chu [7] were among the first to consider this situation and used first-order perturbation analysis to study weak interactions, whereby the shock wave is only slightly perturbed from its base configuration. The first-order theory is adequate only for very small roughness height and does not provide a measure of the *mean* extra forces induced by roughness since for zero mean height the first-order theory predicts zero mean forces. Progress can be made by considering high-order perturbation theory in conjunction with stochastic numerical simulations in order to study the effect of *large* and *fine* random roughness on shock dynamics. An intriguing experimental finding published in the Russian literature [8] suggests that roughness enhances lift in airfoils; this was later confirmed by other experimental studies in the USA [9], but the highest speeds tested were below the supersonic regime.

In this Letter, we revisit the classical aerodynamical problem of supersonic flow past a wedge but we consider random surface roughness on the wedge. We employ a new model for representing the random surface roughness as a stochastic process, and present results for the forces on the wedge based on second-order stochastic perturbation analysis for small roughness and on stochastic numerical simulations for small and large roughness.

We consider a small strip of roughness with zero *mean* and length d around the wedge, as shown in Fig. 1, while the rest of the wedge is smooth. Because of the finite length of the roughness and the effects of boundaries, standard covariance kernels for roughness cannot be used to model this configuration. To this end, we obtain the nondimensional random roughness of correlation length A as a stochastic process $h_m(x;\xi)$ from the solution of the following fourth-order differential equation with stochastic right-hand side [10], of the form

$$\frac{d^4 h_m}{dx^4} + k^4 h_m = f(x), \tag{1}$$

where x is along the wedge and is normalized by the roughness length d, $k = \frac{d}{A}$, and the random forcing term $f(x)$ is *white noise* satisfying: $\mathbb{E}[f(x_1)f(x_2)] = \delta(x_1 - x_2)$, where $\mathbb{E}[\cdot]$ denotes the expectation. The solution is

$$h_m(x;\xi) = \sum_{n=1}^{\infty} \frac{1}{(\Lambda_n^4 + k^4)} \psi_n(x)\xi_n(\omega), \tag{2}$$

where $\psi_n(x) = \cos\Lambda_n x - \cosh\Lambda_n x - \frac{\cos\Lambda_n - \cosh\Lambda_n}{\sin\Lambda_n - \sinh\Lambda_n} \times (\sin\Lambda_n x - \sinh\Lambda_n x)$, Λ_n is obtained by solving $\cos\Lambda_n \cosh\Lambda_n = 1$, and $\{\xi_n(\omega)\}$ (ω is a random event) is a set of uncorrelated random variables with zero mean and unit variance. We have investigated different probability density functions, but here in the numerical results we use *uniform* random variables $\xi_n \in [-\sqrt{3}, \sqrt{3}]$. We also define the nondimensional roughness height (distance from the smooth surface) as

$$y(x;\omega) = \epsilon h(x;\omega) = \epsilon \frac{h_m}{\mu}, \tag{3}$$

where y is normalized by the roughness length d. Also, $\mu = \max_x[\sigma(h_m)]$, $\epsilon = \max_x[\sigma(y)]$, while σ represents the standard deviation.

In order to investigate the effect of roughness granularity, we study three different nondimensional correlation lengths $A/d = 1$, $A/d = 0.1$, and $A/d = 0.01$. These values determine the number of random dimensions, N, that are required for accurate representation of the random roughness in the expansion of ψ of Eq. (2). Here, we obtain N by assuming that the truncated spectrum covers 90% of the entire spectrum. We arrived at this criterion after considerable testing. If the number of random dimensions is not sufficient, oscillations are observed for both the mean and the variance. For the results we present in this Letter

 © 2007 The American Physical Society

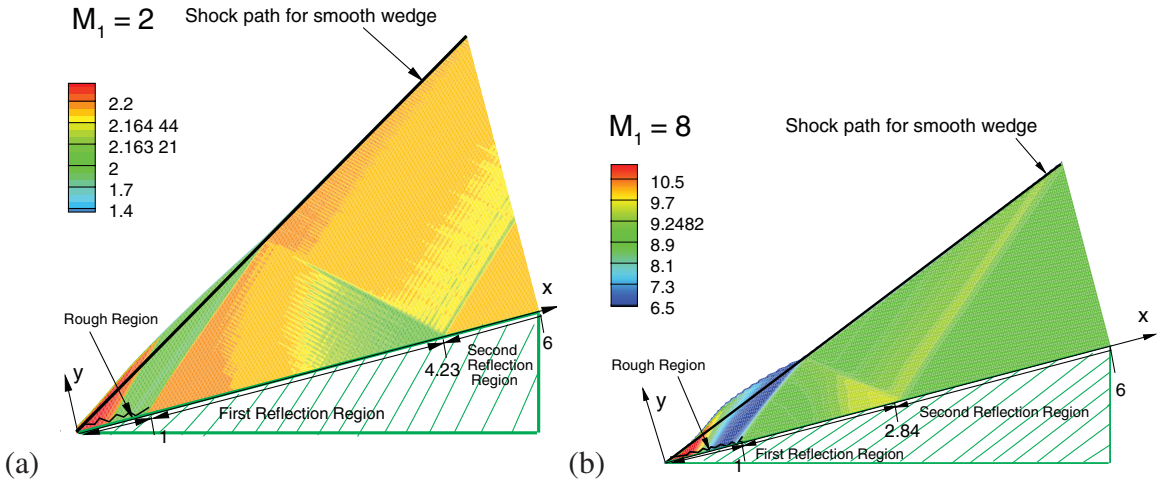

FIG. 1 (color). Flow structure (flow is from left to right): Pressure contours (one realization) for (a) $M_1 = 2$ and (b) $M_1 = 8$ (the pressure contours for $M_1 = 8$ are stretched 4 times perpendicular to the wedge surface for visualization purposes). ($\epsilon = 0.01$ and $A/d = 0.1$).

we have found that $N = 2$ is required for $A/d = 1$, $N = 12$ for $A/d = 0.1$ and $N = 60$ for $A/d = 0.01$.

In order to apply stochastic perturbation analysis, we assume that: (i) The random wedge roughness is small, and correspondingly the perturbation of the shock slope is small. (ii) The oblique shock is attached to the wedge. (iii) The flow between the shock and the wedge is adiabatic. The domain of solution is between the perturbed shock and the wedge surface, and we employ the Rankine-Hugoniot conditions to obtain the flow state after the shock [5]. In first-order perturbation theory, the shock and wedge boundary conditions are imposed at the unperturbed shock location and at the smooth wedge surface. However, in the second-order theory, these conditions are imposed at the *perturbed surfaces* in an iterative manner in order to account for the correct perturbed shock location [11].

Clearly, the perturbed lift has a *mean* value $\propto \epsilon^2$ whereas the corresponding standard deviation scales $\propto \epsilon$. The first-order theory predicts zero mean of perturbed lift since the assumed roughness has zero mean. In [11] (see also online material) we derive detailed scaling laws for these quantities as well as the statistics of the shock path. We summarize here the results for the perturbed wall pressure distribution, Δp_w, for the two extreme cases of correlation length A:

$$A/d \ll 1\text{: } \mathbb{E}[\Delta p_w] \propto \epsilon^2 \mathbb{E}\left[\left(\frac{\partial h}{\partial x}\right)^2\right] \propto \epsilon^2 (A/d)^{-2},$$

$$\sigma(\Delta p_w) \propto \epsilon \sigma\left(\frac{\partial h}{\partial x}\right) \propto \epsilon (A/d)^{-1},$$

$$A/d \gg 1\text{: } \mathbb{E}[\Delta p_w] \propto \epsilon^2 \quad \text{and} \quad \sigma(\Delta p_w) \propto \epsilon,$$

where $\mathbb{E}$ and σ denote mean value and standard deviation, respectively. These results show a strong dependence of the perturbed wall pressure on the granularity of the roughness for small correlation length but no dependence at all for large correlation length. The perturbed lift force on the wedge follows similar scaling laws for the mean, but the standard deviation is different. For example, in the small correlation limit the variance of the perturbed lift is independent of A/d.

Next, we present results based on perturbation analysis and on stochastic numerical simulations. We consider the following conditions: The semi-infinite wedge, see Fig. 1, is truncated after $x = 6$ while the rough region is $x \in [0, 1]$ (x is normalized by the roughness length d); the angle of the unperturbed shock is $\chi_0 = 45°$ ($M_1 = 2$); $\chi_0 = 20.5755°$ and the angle of the wedge is $\theta_0 = 14.7436°$. We consider two values of the inflow Mach number, i.e., $M_1 = 2$ and $M_1 = 8$. All the physical quantities can be obtained from the Rankine-Hugoniot relations; hence, the outflow boundary conditions can be set up accurately. In the simulations, we employ a fifth-order weighted essentially nonoscillatory scheme [12] for spatial discretization with 1000×1000 grid points in the domain $[0, 6] \times [0, 4]$. The stochastic simulations are based on a probabilistic collocation method and multidimensional integration using sparse grids to deal with many dimensions (up to 12); see [11,13].

Typical pressure contours corresponding to one realization for $M_1 = 2$ and $M_1 = 8$ are presented in Fig. 1. A reflection of Mach waves at the wedge surface is observed in both cases, with the reflection point for $M_1 = 8$ being closer to the wedge apex than for the $M_1 = 2$ case. In particular, the reflection splits the wedge [0,6] into three regions, namely: roughness region, first reflection region, and second reflection region, as marked in Fig. 1; these boundaries are predicted by the theory for small ϵ [11]. In the rough region, the pressure contours are all distributed from high (at the apex) to low (at the end of roughness) for

both cases. However, in the first reflection region, the pressure contours are distributed in the opposite ordering for $M_1 = 2$ and $M_1 = 8$; i.e., for $M_1 = 2$ the pressure is from high to low whereas for $M_1 = 8$ the pressure is from low to high.

Next, we present results for the *mean* of the perturbed normalized lift force for $M_1 = 2$ and $M_1 = 8$, respectively, in Figs. 2(a) and 2(b) as a function of the distance from the wedge apex, for roughness amplitude $\epsilon = 0.003$ and $\epsilon = 0.1$, and correlation length $\frac{A}{d} = 0.1$ and $\frac{A}{d} = 1$. For roughness amplitude $\epsilon = 0.003$, the numerical results based on the full solution of the stochastic nonlinear Euler equations agree well with the second-order stochastic perturbation solutions (denoted as "Analytical Soln" in the plot), thus verifying the ϵ^2 dependence. However, for roughness amplitude $\epsilon = 0.1$, the numerical solution deviates significantly from the theory, leading to a scaling $\propto \epsilon^c$ with $1 < c < 2$. There seems to be a qualitative flow change for large roughness height as well, with the perturbed lift force being almost constant beyond the roughness region. This can be explained by the significant distortion of the characteristic lines that lead to a large variation of the location of the reflection point on the wedge for different realizations. This, in turn, will result in an *averaging out* effect in the mean solution with no discernible reflection region anymore. The enhanced-lift force generated due to roughness can be significant and of the same order of magnitude as the lift of the base flow (smooth wedge). Moreover, within the rough region strictly positive mean lift forces are observed for both $M_1 = 2$ and $M_1 = 8$ cases and are increasing significantly both with respect to Mach number and also with d/A; the latter implies that a large lift force can be obtained for *fine* granularity roughness. For large roughness (large ϵ) the perturbed lift increases almost monotonically with the distance to the apex but large variations occur, especially for $M_1 = 8$, beyond the roughness region for small ϵ.

Finally, we summarize the analytical and numerical results in the plot of Fig. 3, where we present the perturbed nondimensional mean lift, $\Delta L(1)$, integrated from the apex to the end of the roughness, $x \in [0, 1]$, as a function of A/d and ϵ at inflow Mach number $M_1 = 8$. The curvilinear surface in Fig. 3 represents the region of validity of the stochastic perturbation analysis. We see that the validity region for $\frac{A}{d} = 0.01$ is much smaller than the validity region for $\frac{A}{d} = 1$, but there is no difference between the validity region for $\frac{A}{d} = 1$ and $\frac{A}{d} = 10$. On the curvilinear surface, for fixed $\frac{A}{d}$, $\frac{\mathbb{E}[\Delta L(1)]}{\epsilon^2}$ is independent of ϵ, which means that for small roughness amplitude the mean of the perturbed mean lift scales $\propto \epsilon^2$. We also observe the scaling $\propto (A/d)^{-2}$ in the small A/d region (slope of -2 in the plot). For large ϵ (lines with cubic symbols in the plot), the numerical results deviate from the ϵ^2 scaling, as also shown in Fig. 2.

We have so far established that the *mean lift* increases with the Mach number and more importantly by refining the roughness. However, the corresponding perturbed *mean drag force* increases similarly, so, from the practical standpoint, optimization studies should be performed to select the proper roughness that maximizes the *lift-to-drag* ratio. For small ϵ, perturbation analysis can be used to formulate this stochastic inverse problem in terms of $h(x, \xi)$. We have done this by postulating simple profiles of the form $(1 - x)^b x\xi (0 \le x \le 1)$ and obtaining the range of the deterministic parameter b that gives maximum lift-to-drag ratio, also confirming that this ratio is larger than the ratio of the smooth wedge. However, for more general profiles of random roughness a numerical optimization approach should be employed. It is also important for such considerations to take into account the fluctuations in the lift, quantified by the standard deviation $\sigma(\Delta L)$. The perturbation analysis reveals a scaling $-\frac{\mathbb{E}[\Delta L]}{\sigma(\Delta L)} \propto \epsilon (A/d)^{-2}$, since $\sigma(\Delta L)$ is independent of A/d. On the

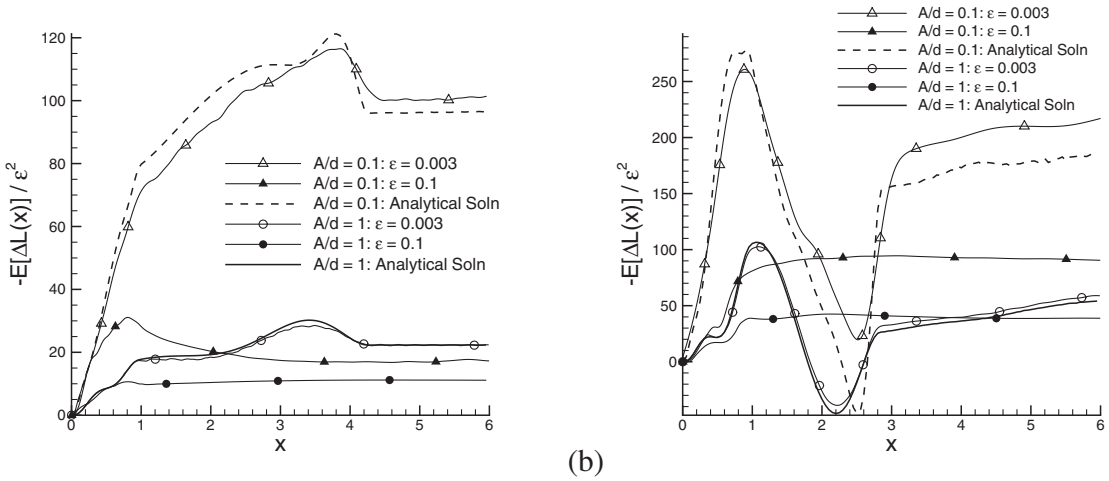

FIG. 2. Enhanced-lift force: Distribution of the perturbed mean lift along the wedge surface (the wedge apex is at $x = 0$). (a) $M_1 = 2$ and (b) $M_1 = 8$. (The lift is normalized by $P_2 d$, where P_2 is the pressure after the shock of the corresponding smooth wedge.)

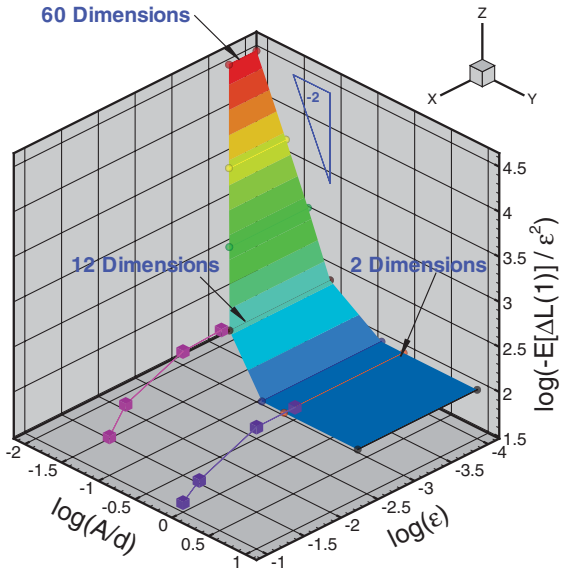

FIG. 3 (color). Summary of analytical and numerical results. Plot of the mean of the perturbed nondimensional lift as a function of A/d and ϵ. $M_1 = 8$. The color surface corresponds to the region of validity of perturbation theory. The lines with cubic symbols correspond to stochastic simulations for large ϵ.

other hand, numerical simulations for $\epsilon \geq 0.01$ show that $-\frac{\mathbb{E}[\Delta L]}{\sigma(\Delta L)} > 1$ for $A/d = 0.1$, and this ratio becomes much larger for fine granularity roughness ($A/d \ll 1$).

We can readily extend our results to a full semi-infinite wedge, where the upper surface is smooth whereas the lower one has a strip of random roughness of the type that we studied in this Letter. A *net* mean lift will be obtained, while due to symmetry and inviscid assumptions, there will be no net lift for a full semi-infinite wedge with both smooth surfaces. Clearly, these ideas can be extended to actual supersonic airfoils, where it will be beneficial to mount on the under side of the airfoil a skin of fine random roughness whereas the suction side should be either maintained smooth or rough but with much larger roughness granularity.

Finally, we remind the reader that in this study we refer to the *wave* lift and drag and did not take into account the subtle structural changes near the wall due to viscous stresses nor did we consider the real gas effect [3]. We also note that our results are based on a stochastic analysis that employs random variables of compact support. In this case, the mean and standard deviation of pressure distribution do not depend on the particular probability density function for small ϵ (unlike the higher order moments) but they do depend on it for larger roughness.

This work was supported by the Computational Mathematics program of the Air Force Office of Scientific Research and the National Science Foundation (AMC-SS). Computations were performed on DoD supercomputers.

*glin@dam.brown.edu
†Chau-Hsing_Su@Brown.edu
‡gk@dam.brown.edu

[1] G.-Q. Chen and M. Feldman, Proc. Natl. Acad. Sci. U.S.A. **102**, 15 368 (2005).
[2] J. Olejniczak, M. J. Wright, and G. V. Candler, J. Fluid Mech. **352**, 1 (1997).
[3] H. Hornung, Annu. Rev. Fluid Mech. **18**, 33 (1986).
[4] J. Von Neumann, Collected Works (Pergamon, New York, 1963), Vol. 5.
[5] H. W. Liepmann and A. Roshko, *Elements of Gas Dynamics* (Wiley, New York, 1957).
[6] M. J. Lighthill, Philos. Mag. **40**, 214 (1949).
[7] B.-T. Chu, J Aeronaut Sci **19**, 433 (1952).
[8] N. N. Vorobiev, Sov. Phys. **36**, 373 (1991).
[9] R. C. Ranzenbach, M. T. Beierle, and J. D. Anderson, Jr., *15th AIAA Applied Aerodynamics Conference* (AIAA, Atlanta, GA, 1997).
[10] C.-H. Su and D. Lucor, J. Comput. Phys. **217**, 82 (2006).
[11] G. Lin, Ph.D. thesis, Brown University, 2007; See EPAPS Document No. E-PRLTAO-99-012736 for a supplementary figure and appendices. For more information on EPAPS, see http://www.aip.org/pubservs/epaps.html.
[12] G.-S. Jiang and C.-W. Shu, J. Comput. Phys. **126**, 202 (1996).
[13] D. Xiu and J. S. Hesthaven, SIAM J. Sci. Comput. **27**, 1118 (2005).